RSC Advances

ROYAL SOCIETY OF CHEMISTRY

www.rsc.org/advances

Journal Name

RSCPublishing

ARTICLE

Palladium Nanoparticles on Noncovalently Functionalized Graphene-based Heterogeneous Catalyst for the Suzuki–Miyaura and Heck-Mizoroki Reactions in Water

Cite this: DOI: 10.1039/x0xx00000x

Received 00th January 2012,
Accepted 00th January 2012

DOI: 10.1039/x0xx00000x

www.rsc.org/

Vittal Sharavath and Sutapa Ghosh*

We describe here a methodology to synthesize a reusable heterogeneous catalyst based on palladium nanoparticles (Pd NPs) supported on noncovalently functionalized graphene using 1-pyrene carboxylic acid. This can be used efficiently for Suzuki-Miyaura and Heck-Mizoroki reactions in water up to five cycles, providing excellent yields with high selectivity of cross coupled products. It is also useful for more challenging substrates like electron-rich and electron-poor bromoarenes and chloroarenes which resulted good isolated yields (alkenes and biphenyls) in pure water. Use of functionalized graphene in the catalyst preparation improved the dispersion of it in water medium and also acted as a stabilizing agent for the Pd NPs. Percentage of metal loading in the catalyst and its thermal stability were determined by Inductively Coupled Plasma Atomic Emission Spectroscopy and Thermo gravimetric analysis respectively. The composite formation was confirmed by X–ray diffraction pattern, Fourier Transform Infrared Spectroscopy and Raman spectroscopy. The surface elemental composition with oxidation state was determined by UV-Visible and X–ray photoelectron spectroscopy. The size and morphology of Pd NPs on the functionalized graphene sheets was directly observed by Transmission Electron Microscopy.

Introduction

In recent years, graphene nanosheets (GNS) have aroused significant interest due to their huge theoretical specific surface area, high chemical stability, low manufacturing cost and high electron mobility. Because of these interesting properties, GNS are promising candidates for use in super capacitors, batteries, photo catalysis and photovoltaics.[1-14] GNS are also useful as promising 2D support layers for metallic NPs in heterogeneous catalysis. As metal nanoparticles suffer from the problems of separation, recycling, and

deactivation via the aggregation of nanoparticles during reaction, it is highly desirable to deposited metal NPs on solid supports for their use in organic transformations to overcome these problems. Metal nanoparticles have also been supported on surfactants, polymers or various types of ligands, or organic and inorganic substrates, such as carbon materials, silica or zeolites.[15,16] The main advantage of this solid supported catalyst is that the solid support does not allow the metal NPs to dissociate from the solid surface, which would result in higher stability of the active metal species. Solid-supported catalysts also offer easy isolation of the catalyst from reaction mixtures by simple filtration, decantation or magnetic separation as reusable catalysts.[17,18]

The use of GNS or graphene oxide (GO) or functionalized graphene based materials serving as a support for palladium nanoparticals (Pd NPs) are especially important for their extensive catalytic applications in organic transformations such as carbon-carbon (C-C) cross coupling reactions.[7-13,19-29] Suzuki–Miyaura and Heck-Mizoroki C-C cross coupling reactions are most useful methods for various industrially important organic transformations. These are also having promising academic interest. Due to their wide range of applications for C–C bond formation, there is considerable interest in this area with a focus directed towards the development of more efficient and recyclable catalysts for industrial applications in environmentally benign processes.[15,16, 30-39] Graphene supported Pd NPs have been reported to be highly active catalysts for not only C-C cross coupling reactions but also for some other catalytic applications such as ammonia borane dehydrogenation,[40] aerobic oxidation of aromatic alcohols,[10] CO oxidation,[41] selective oxidation of methanol and formic acid oxidation,[42,43] non enzymatic glucose sensor,[44] ethanol electro catalysis oxidation,[45] chemo selective reduction of α,β--unsaturated carbonyl compounds[46] and reduction of aromatic nitro compounds[47,48]

Volatile and highly inflammable organic solvents are used in most of the organic reactions, which are a major cause of ecological contamination.[49] However, it is often difficult to avoid the use of such solvents as they are vital in various stages of reactions for isolation of product from reaction mixture. The ideal solution is to use a "green solvent" which does not pollute the environment.[15] One approach is to utilize water dispersible (hydrophilic) micellar Pd catalysts, which are suitable for aqueous phase reactions in organic transformations.[50-522]

In this paper, we have demonstrated the synthesis of an efficient and reusable heterogeneous catalyst based on Pd NPs supported on graphene which is noncovalently functionalized by 1-pyrene carboxylic acid (PCA-GNS-Pd). Further, PCA-GNS-Pd catalyst is used for various organic transformations through sustainable and greener pathways. This catalyst is amphiphilic due to the hydrophobic nature of polyaromatic carbon groups (graphene and pyrene moieties) and hydrophilic carboxylate groups present on pyrene carboxylic acid. Because of the carboxylic groups present in this catalyst, the intercalation and sorption of Pd NPs on the PCA-GNS support during the reduction of Pd^{+2} ions and further the association of organic substrates during the catalytic reaction due to non covalent interaction of PCA are possible. This leads to easy dispersion of catalyst in water and therefore the use of organic solvent is avoided during the reaction. The main advantage of the PCA-GNS-Pd catalyst is that it can be used in environmentally benign solvent such as water and effectively reusable up to five successive cycles. we have demonstrated synthesis of another efficient Graphene-based Heterogeneous Palladium Catalyst for the Suzuki–Miyaura and Heck-Mizoroki Reactions in Water. This heterogeneous catalyst system exhibits significant activity towards aryl bromides as well as less reactive aryl chlorides, which are more readily available and less expensive. Good to excellent yields and

high selectivity of the cross coupled products were obtained with low catalyst (0.2 mol %) loading. We hope that this work provides a important step toward the development of green technologies for organic synthesis.

2.Experimental Section

2.1. Synthesis of noncovalent functionalized graphene (PCA-GNS)

Graphite Oxide (GO) was synthesized from natural graphite powder by modified Hummers method[53] and noncovalent functionalized graphene was prepared by reported method.[54] In a typical experiment, 100 mg GO was dispersed in 200 mL of deionized water by sonication for 30 min and then centrifuged at 1000rpm for 3 min. To the obtained supernatant, 100 mg (0.5 mmol*L^{-1}) of NaOH and 125 mg (0.1 mmol*L^{-1}) of 1-pyrenecarboxylic acid were added followed by hydrazine monohydrate (500 μL, 2 mmol*L^{-1}). The mixture was then stirred at 80°C for 24 h. The final product was isolated by centrifugation at 3000 rpm for 10 min and washed with distilled water for five times. The obtained PCA-GNS was dried at 60ºC for overnight.

2.2. Synthesis of noncovalent functionalized graphene supported Pd nanoparticle catalyst (PCA-GNS-Pd)

The PCA-GNS-Pd catalyst was prepared (Scheme 1) as follows: PCA-GNS (100 mg) was ultrasonicated in absolute ethanol (EtOH) (75 mL) for 30 min. Then $PdCl_2$ (25 mg) was added to the above suspension and refluxed at 80^0 C for 1 h under vigorous stirring. In this case, the EtOH acted both as a solvent and as an in situ reducing agent.[18] After the reaction, the PCA-GNS-Pd catalyst was isolated by centrifugation and washed with distilled water for five times. The obtained catalyst was dried at 60ºC for overnight. Based on the Inductively Coupled Plasma Atomic Emission Spectroscopy (ICP-AES) results, it was confirmed that 10.175 wt% of Pd was loaded on to the PCA-GNS support.

Scheme 1: Preparation of the PCA-GNS-Pd catalyst

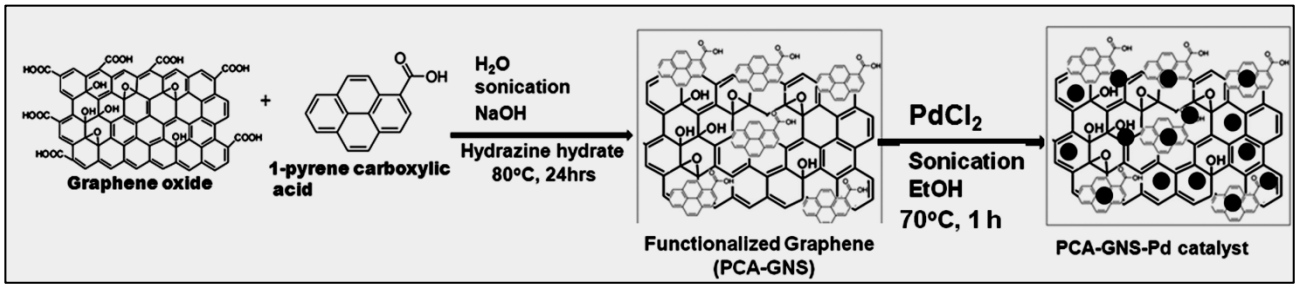

2.3. General procedure for the Suzuki-Miyaura cross coupling reaction

The PCA-GNS-Pd catalyst (3 mg, 0.2 Pd mol% *vs.* halide) was dispersed in 5 mL of H_2O by sonication for 30 min at RT. To this suspension, 1.435 mmol *p*-bromobenzaldehyde, phenylboronic acid (1.722 mmol) and Na_2CO_3 (2.153 mmol) were added and the reaction mixture was stirred at 90ºC for required time. The reaction was monitored by TLC (thin-layer chromatography) and the product was extracted with ethyl acetate (5 × 15 mL). The obtained organic extracts were dried over anhydrous Na_2SO_4 and the crude product was purified by column chromatography (silica, n-hexane/ethyl acetate (95:5)). The isolated products were confirmed by ^{1}H and ^{13}C NMR spectroscopy.

2.4. Heck-Mizoroki cross coupling reaction

To the dispersed aqueous suspension of Pd catalyst (3 mg, 0.2 Pd mol% *vs.* aryl halide), *p*-bromobenzaldehyde (1.435 mmol), styrene (1.722 mmol), Na_2CO_3 (2.153 mmol) and tetrabutyl ammonium bromide (TBAB) (2.153 mmol) were added and the reaction mixture

was stirred at 90ºC for required time. All reactions were monitored by TLC. The isolation procedure was similar to Suzuki-Miyaura reaction.

2.5. Characterization methods

X-ray diffraction (XRD) pat-terns were taken in reflection mode on a Rigaku MiniFlex tabletopX-ray diffractometer using a Cu K _ source (λ). Powder XRD patterns were recorded on a Siemens (Cheshire, UK) D5000 X-ray diffract meter by using Cu Kα (l=1.5406m) radiation at 40 kV and 30 mA equipped with a standard monochromatic equipped with a Ni filter radiation with a scan rate of 1.0 s/step and step size of 0.02° at 298 K over the range of $2\theta = 10$ to 60°. UV-Vis spectra were recorded on a Varian Cary 5000 UV-VIS-NIR spectrophotometer in the range 200-800 nm. FT-IR (Fourier transform infrared) spectra were recorded on a BRUKER ALPHA T spectrometer from 4000 cm^{-1} to 400 cm^{-1} as KBr disks. A Thermo Electron Inductively Coupled Plasma Atomic Emission spectrometer (ICP-AES) (Model, IRIS Intrepid IIXDL) was used for determining the metal composition of the samples. X-ray photoelectron spectroscopy (XPS) spectra were recorded on a KRATOS AXIS 165 with a dual anode (Mg and Al) apparatus using the Mg Kα anode. A Transmission Electron Microscope (Philips Tecnai-12 FEI, operating at 80–100 kV) was used to investigate the morphology and size of the particles. Confocal Micro-Raman spectra were recorded at room temperature in the range of 50-4000 cm^{-1} using a Horiba Jobin-Yvon Lab Ram HR spectrometer with a 17 mW internal He-Ne (Helium-Neon) laser source (excitation wavelength 632.8 nm). ^{1}H and ^{13}C NMR spectra were recorded on a Bruker Avance spectrometer (300 or 500 MHz) in $CDCl_3$ using TMS as an internal standard, unless stated otherwise. All reagents were commercially available and used without purification.

3.Results and Discussion

3.1 X–ray diffraction analysis of the PCA-GNS-Pd catalyst

Fig. 1 shows the X–ray diffraction (XRD) pattern of PCA-GNS (a) and the PCA-GNS-Pd catalyst (b). The functionalised graphene showed a very strong (002) peak at 2θ = ~25.9º and a weak (101) peak at 2θ =~42.8º. These broad peaks clearly indicate the presence of single or few layered structure of GNS. A small peak at 2θ = 17.9º may be due to PCA embedded in GNS sheets.[54]

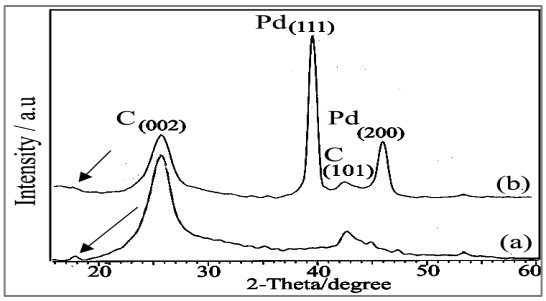

Fig. 1. XRD patterns for (a) PCA-GNS and (b) PCA-GNS-Pd catalyst.

The peaks at 2θ value of 40.2° and 46.6° (Fig. 1b) are indexed to the (111) and (200) crystal planes of face-centred cubic (fcc) lattice pertaining to Pd NPs. The broad diffraction peak at 2θ = 40.2° clearly indicates that the Pd NPs formed are of small size. The average crystalline size of the prepared Pd NPs was estimated to be ~9.3 nm using Scherrer's equation.[53]

3.2. TEM analysis of the PCA-GNS-Pd catalyst

Fig. 2 shows the transmission electron microscopy (TEM) images of PCA-GNS, freshly prepared PCA-GNS-Pd catalyst and PCA-GNS-Pd after three reaction cycles. From the Fig. 2a, it is clear that PCA-GNS is having sheet like structure. TEM images of freshly prepared PCA-GNS-Pd catalyst (Fig. 2b and Fig. 2c) indicate that Pd NPs are deposited with different particle size distribution on the graphene

Journal Name

RSCPublishing

ARTICLE

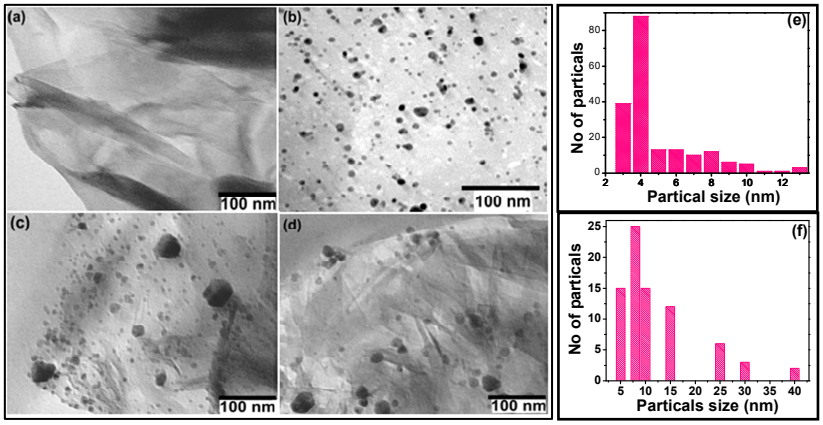

Fig. 2. TEM images of PCA-GNS sheet (a), freshly prepared PCA-GNS-Pd catalyst (b,c), used PCA-GNS-Pd catalyst after three cycles of the Suzuki reaction (d), particle size distribution analysis of fresh PCA-GNS-Pd catalyst (e) and used PCA-GNS-Pd catalyst after three cycles of Suzuki reaction.

surface with no significant particle aggregation. Further, it is also clear from Fig.2b that the sizes of the Pd NPs are between 3-13 nm which is close to the result obtained from XRD analysis. The TEM image of used PCA-GNS-Pd catalyst after three cycles of the Suzuki reaction is shown in Fig. 2d. The particle size distributions of the fresh and reused (after the three cycles) PCA-GNS-Pd catalysts are shown in fig 2e and fig 2f respectively. It is also clear from fig 2f that the Pd NPs on used catalyst are bigger in size and lesser in number than those on fresh catalyst due to slight agglomeration and leaching of the Pd NPs during the chemical reaction.[30] The leaching of Pd NPs was confirmed by ICP-AES analysis (see recyclable section).

3.3. X–ray photoelectron spectroscopy analysis of the PCA-GNS-Pd catalyst

The oxidation state of the Pd NPs deposited on PCA-GNS surface was assessed by means of X-ray photoelectron spectroscopy (XPS) (Fig. 3). In Fig. 3a, Pd^0 3d peak exhibits a unique doublet with binding energies at 335.3 and 340.8 eV (Δ = 5.3 eV), corresponding to Pd^0 $3d_{5/2}$ and Pd^0 $3d_{3/2,}$ respectively. The XPS spectrum of the catalyst after being recycled for three times (Fig. 3b) in the Heck reaction shows the presence of additional peaks at higher binding energy at 337.0 eV and 343.0 eV (Δ = 6.0 eV) corresponding to Pd $3d_{3/2}$ and Pd $3d_{5/2,}$ demonstrating the presence of $Pd^{(II)}$. This can be attributed to the slight conversion of $Pd^{(0)}$ to $Pd^{(II)}$ which most likely indicates the complexation of Pd NPs with oxygen functionalities of the PCA-GNS support by forming Pd-O linkages.[18,55,56]

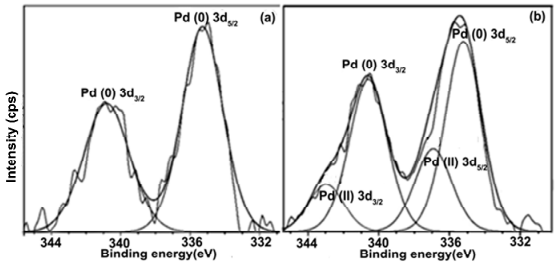

Fig. 3. XPS narrow scan for Pd (a) in fresh PCA-GNS-Pd and (b) used PCA-GNS-Pd after three cycles of the Heck reaction.

3.4. Raman spectroscopic analysis of the PCA-GNS-Pd catalyst

Fig. 4 shows the Raman spectra of GO, PCA-GNS and PCA-GNS-Pd samples. From the figures, one can see that these three materials exhibited two bands at ca. 1566 cm^{-1} and 1327 cm^{-1}, corresponding to the G band and D band of graphitic nanostructures, respectively. It can be noted that the G band is assigned to the E2g phonon of the sp^2 carbons and the D band is a breathing mode of the κ-point phonons of A1g symmetry. The Raman spectra of GO, PCA-GNS and PCA-GNS-Pd are shown in Fig4a, Fig 4b and Fig4c respectively. These figures display an obvious blue shift of the D band from ~1327cm^{-1} (Fig 4a) to ~1333cm^{-1} (Fig 4b) and further to ~1340cm^{-1}(Fig 4c). This blue shift is observed due to the introduction of large number of structural defects during surface functionalization of GO by 1-pyrene carboxylic acid groups under vigorous reaction conditions and further incorporation of Pd NPs by reduction of Pd^{+2} under mild chemical condition in ethanol. The spectra of GO,PCA-GNS and PCA-GNS-Pd also show G band at ~1566, cm^{-1}~1590cm^{-1} and ~1599cm^{-1}, respectively. In each case, the G band is blue shifted compared to GO (~1566 cm^{-1}).

The D band and G band indicate the order/disorder of the graphite edge and the graphitic stacking structure respectively. High D/G intensity ratios are associated with high degree of disorder/exfoliation. The D/G ratios for GO, PCA-GNS and PCA-GNS-Pd were calculated to be approximately 0.53, 1.08, and 1.15, respectively. This ratio is higher for PCA-GNS / PCA-GNS-Pd compared to GO which significantly indicate the reduction of GO with exfoliation in both cases. Further, D/G is increasing from b to c which clearly indicates chemical interaction between PCA-GNS and Pd NPs with exfoliation during the reaction between PCA-GNS and $PdCl_2$.

We have also observed high-energy second-order 2D-bands for the GO, PCA-GNS and PCA-GNS-Pd samples at ~2648cm^{-1}, ~2566cm^{-1}, and ~2672cm^{-1}, respectively which is associated with the local defects. A 2D band, which is the characteristic band of graphene, is generally used to find out the number of layers of graphene in the material. These 2D bands indicate that the nanosheets contain only a few layers of graphene. . The peak position at 2672 cm^{-1} of the 2D band of PCA-GNS-Pd is nearer to that of a monolayer graphene (2690 cm^{-1}) which confirms further exfoliation of layered structure after Pd NPs are introduced on PCA-GNS to form composite. [56-59]

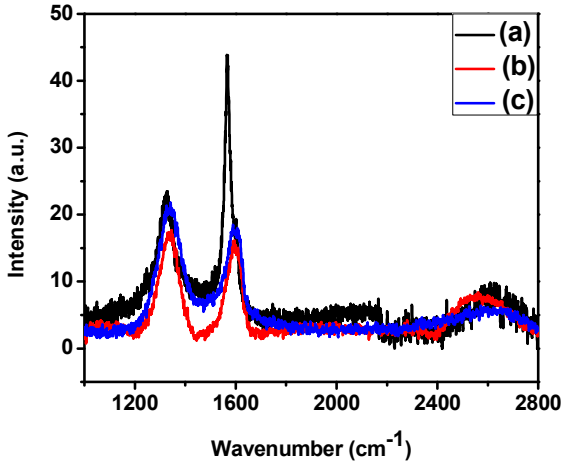

Fig. 4. Raman spectra of (a) GO, (b) PCA-GNS and (c) PCA-GNS-Pd catalyst.

3.5. Fourier Transform Infrared Spectroscopy analysis of the PCA-GNS-Pd catalyst

The Fourier Transform Infrared Spectroscopy (FT-IR) spectra of the PCA-GNS support and PCA-GNS-Pd catalyst (Fig. 5) show broad absorption signals in the range of 3167-3440 cm^{-1}, attributed to -OH stretching vibrations. Sharp peaks at about 2935 cm^{-1} and 2845 cm^{-1} are due to asymmetric and symmetric stretching vibrations of Ar-H (-CH_2 groups), respectively.[60,61]

The absorption bands in the range of 1000-1160 cm^{-1} are due to O-H bending vibrations.The stretching vibrations for the carboxyl groups, aromatic C=C stretching and asymmetric stretching vibration of COO^- as well as the coupled C-OH asymmetric stretching vibration of graphene are observed at 1740 cm^{-1}, 1554 cm^{-1}, 1670 cm^{-1} and 1390 cm^{-1}, respectively. It is clear from the graph (fig 6a) that, peak intensities due to the C=O, C-O and –OH functional groups are decreased which may be due to the binding of Pd NPs to the PCA-GNS support via the oxygen containing functional groups.[53]

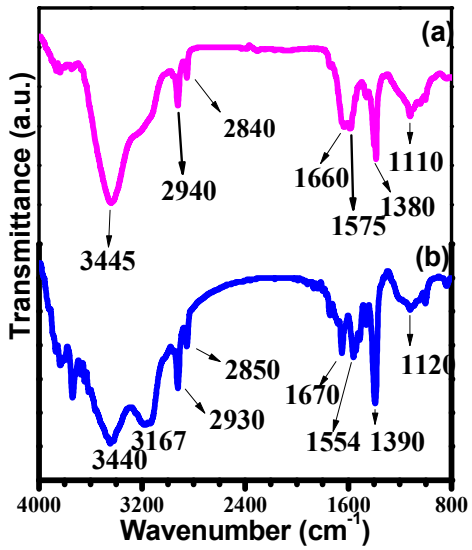

Fig. 5. FT-IR spectra of (a) PCA-GNS-Pd catalyst and (b) PCA-GNS

3.6. UV-Visible spectroscopy analysis of PCA-GNS-Pd catalyst

The reduction process of $PdCl_2$ in the PCA-GNS and ethanol suspension was monitored by UV-Vis spectroscopy, as shown in Fig. 6. The solvent, *i.e.* ethanol, acts as an in situ reducing agent for the Pd salt (Fig. 6a). A peak at 425 nm, corresponding to $Pd^{(II)}$ was present before the start of the reaction and this peak was slowly disappeared after 1 hour, in addition a broad plasmon absorbance extending in to the visible region was observed indicating the complete formation of $Pd^{(0)}$ NPs on PCA-GNS surface (Fig. 6b).[62]

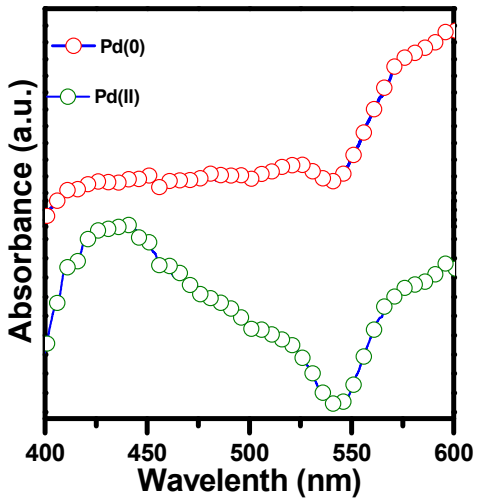

Fig. 6. UV-Visible spectra of $PdCl_2$ and PCA-GNS in ethanol (a) initially, and (b) after 1 hour reflux.

3.7. Thermo gravimetric analysis of the PCA-GNS-Pd catalyst

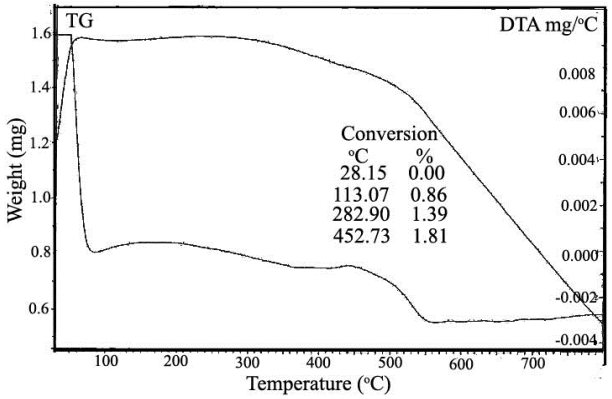

Fig. 7: TG-DTA analysis of PCA-GNS-Pd catalysts.

We have examined the thermal stability of the PCA-GNS-Pd catalyst under nitrogen atmosphere using Thermo gravimetric analysis (TGA). As shown in Fig 7, marginal weight loss (0.86%) is observed only at 113.07ºC .This indicates that the catalyst is thermally stable at 90ºC at which the catalytic reactions are carried out. The insignificant weight loss of the catalyst from 113.07ºC to 452.73ºC

and after that continuous mass loss can be attributed to the evaporation of moisture and degradation of catalyst support in the form of carbon materials such as CO and CO_2 respectively.

3.8. Use of PCA-GNS-Pd Catalyst for C-C coupling reactions

3.8.1. Suzuki-Miyaura cross coupling reaction

Scheme 2. Suzuki reaction of aryl halides with phenylboronic acid by PCA-GNS-Pd

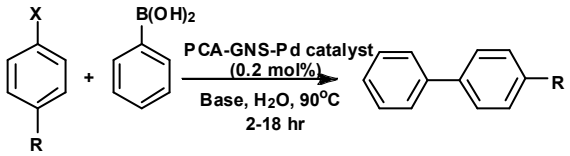

It was demonstrated in previous report that, PCA-GNS was found to have high dispersability and stability in water without forming aggregates.[54,63] Further, the carboxylate groups in the functionalized graphene stabilize the NPs during the reaction in water medium. Due to these advantageous properties, the PCA-GNS-Pd catalyst was tested as a recyclable heterogeneous catalyst in water. The use of water as a solvent also has the advantage of readily dissolving bases, thereby deprotonating the boronic acid and increasing the rate of reaction. Using *p*-bromobenzaldehyde and phenylboronic acid as reagents and a catalyst loading of 0.2 mol% in the presence of inorganic bases such as Na_2CO_3, high yield of coupled product was obtained and was chosen for future reactions. (Table 1, entry 2) (Scheme 2). Under the same conditions, the use of Et_3N as base gave comparable yield.

Various aryl bromides were tested in water using this catalyst for the Suzuki reaction with phenylboronic acid in the presence of Na_2CO_3 and the results were summarised in Table 1 (entries 1-13). The results indicate good to excellent yields of coupled product. Notably there were no obvious effects on yield when aryl bromides containing electron-donating or electron-withdrawing substituents were used.

Table 1. Suzuki-Miyarua coupling of aryl halides with phenylboronic acid by PCA-GNS-Pd catalyst[a].

Entry	R_1	X	Yield (%)[b]	Time(h)
1	H	Br	97	2
2	*p*-CHO	Br	96, 98[d]	2.5, 2.5[d]
3	*p*-OMe	Br	85[f]	6
4	*p*-OH	Br	90	4
5	*p*-Me	Br	85	7
6	*2,4*-OMe	Br	80	9
7	*1*-naphthyl[(d)]	Br	85	6
8	*2*-pyridyl	Br	80	5
9	*3*-pyridyl	Br	82	4.5
10	*5*-pyrimidine	Br	80	4.5
11	*m*-NO_2	Br	90[e],75[c]	2[e], 12[c]
12	H	Cl	80	15
13	*p*-CHO	Cl	85	18
14	*2*-pyridyl	Cl	60	15
15	*3*-pyridyl	Cl	67	15
16	*m*-NO2	Cl[e]	75	15
17	*p*OH	Cl	70	10
18	*2,4*-OMe	Cl	65	15

[a]Reaction conditions: aryl halide (1.435 mmol), phenylboronic acid (1.722 mmol) Na_2CO_3 (2.153 mmol), water (5 mL), PCA-GNS-Pd (3 mg, 0.2 mol%) ol% Pd vs. halide), heated to 90 °C.

[b] Isolated yield.

[c] PCA-GNS-Pd (3 mg, 0.6 mol% Pd vs. halide) was used.

[d] Isolated yield and time using Et_3N as base.

[e] 4-cyanophenylboronic acid was used instead of $PhB(OH)_2$.

[f] 2-napthylboronic acid was used instead of $PhB(OH)_2$.

Whereas moderate yields were obtained when tested with electron-rich and electron-poor aryl chlorides (Table 1, entries 12-18), at a longer reaction times. Further, the coupled products obtained with the sterically hindered aryl halide substrates were also in moderate to good yields (Table 1, entries 6, 8, 14, 18). The Pd-reduced Graphene oxide and Pd-GO nano composites are having lower catalytic activity towards chloro and bromo arenes in water than the PCA-GNS-Pd nanocomposites.[26-29]

3.8.2. Heck-mizoroki cross coupling reactions

S

cheme 3. Heck-Mizproki coupling reaction of aryl halides with styrene byPCA-GNS-Pd

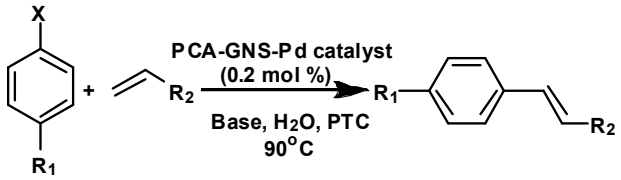

The utility of the PCA-GNS-Pd catalyst was further evaluated for C−C bond forming processes, namely the Heck-Mizoroki cross coupling of aryl bromide or chloride with an olefin (Scheme 3) in pure water with 0.2 mol% of PCA-GNS-Pd as catalyst, and the results are shown in Table 2. By optimising the coupling reaction between p-bromobenzaldehyde and styrene in the presence of TBAB (Phase Transfer Catal yst (PTC)) and Na_2CO_3 (Table 2, entry 4),

Table 2. Heck-Mizoroki coupling of aryl halides with Styrene (or) Olefin by PCA-GNS-Pd catalyst [a.]

Entry	R^1	R^2	X	Yield (%)[b]	Time (h)
1	H	Ph	Br	85,0[c]	12, 20[d]
2	Me	Ph	Br	71	15
3	Cl	Ph	Br	70	13
4	CHO	Ph	Br	90, 50[c]	18, 30[c]
5	OMe	Ph	Br	75	20
6	H	Ph	Cl	75	18
7	Me	Ph	Cl	70	24
8	CHO	Ph	Cl	60	20
9	OMe	Ph	Cl	55	30
10	CF3	Ph	Br	70	15
11	H	COOH	Br	82	5
12	H	COOMe	Br	90	15
13	H	$COOC_4H_9$	Br	92	12
14	NO_2	COOH	Br	85	12
15	CHO	COOH	Br	81	15
16	OMe	COOH	Br	68	18
18	NO_2	COOH	Cl	45	22
19	CHO	COOH	Cl	41	24

[a] Reaction conditions: aryl halide (1.435 mmol), styrene (1.722 mmol) Na_2CO_3 (2.153 mmol), TBAB (2.153 mmol), water (5 mL), PCA-GNS-Pd (3 mg, 0.2 mol% Pd vs. halide), heated to 90°C.

[b] Isolated yield.

[c] PCA-GNS-Pd (3 mg, 0.6 mol% Pd vs. halide) was used.

[d] Isolated yield and reaction time in the absence of TBAB

as a model reaction. A series of reactions were carried out. The results showed the complete conversion of substrates with high isolated yield of the cross coupled product (Table 2). Until recently, the use of Pd NPs supported on carbon-based materials as catalysts for the coupling of sterically challenging electron-rich and electron-poor aryl chlorides in aqueous media was very uncommon.[63] We have demonstrated that the PCA-GNS-Pd catalyst provides broader possibility than the reported catalysts with respect to the coupling of aryl chloride and aryl bromides (under optimized conditions). The electron deficient substrates such as 4-chlorobenzaldehyde and 4-bromobenzaldehyde when coupled with styrene and olefins respectively gave good yields of products (Table 2, entries 4, 8, 15 and 19). The PCA-GNS-Pd also successfully catalyzed the Heck reactions of electron rich 4- chloroanisole and 4-bromoanisole with styrene and olefins respectively (Table 2, entries 5, 9 and 16) with good to moderate yields. Further, moderate yields were obtained with more challenging substrates, for example, the coupling of electron-deficient aryl chlorides with acrylic acid (Table 2, entries 18, 19).

4. Recyclability of the PCA-GNS-Pd catalyst

The coupling of *p*-bromobenzaldehyde with phenylboronic acid and styrene was used as model reactions to monitor the recyclability of the catalyst in the Suzuki-Myaura, Heck-Mizoroki cross coupling reactions, respectively. Details of reaction conditions and work-up procedures are given below. The conversion percentage of the cross coupled product, recycle numbers and time required for that are shown in fig 8 and table 3.

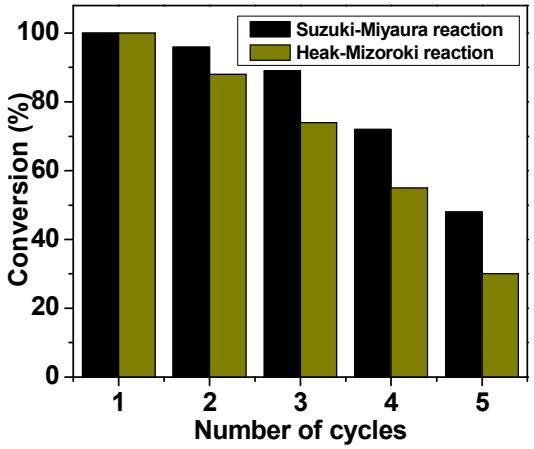

Fig 8: Recyclability test for Suzuki- miyaura and Heak-Mizoroki cross coupling reaction.

After completion of the reaction, the coupled product was repeatedly extracted from the reaction mixture with ethyl acetate. The catalyst was recovered by centrifugation and washed with cold EtOH, water and acetone. The obtained catalyst was dried at 60ºC for overnight. The dried catalyst was then subjected to further coupling reaction. It is found that slight decrease in activity was observed gradually over five successive runs due to the leaching of Pd NPs from the support during the reaction and their agglomeration on the catalyst support. Hot filtration test was performed to conform this for the reaction of 4-bromobenzaldehyde with phenylboronic acid in the presence of PCA-GNS-Pd catalyst in pure water at 90°C. The reaction mixture was cooled down to room temperature after 40 min of the reaction time. The analysis of the reaction mixture showed that the isolated yield of cross coupled product is 30%. When the reaction further proceeds with the filtrate, 65% of cross coupled product has been observed, however, with increased reaction time up to ~20 hrs. ICP-AES analysis showed that there was only a 0.25 wt % loss of Pd in the used catalyst after three cycles of the Suzuki-Miyaura reaction compared to that in the original

catalyst. It is already conformed by the TEM image of the catalyst collected after three cycles (see Fig 2d).

Table 3. Reusability of PCA-GNS-Pd in the Suzuki-Miyaura and Heck-Mizoroki coupling reactions.

No of cycles	1	2	3	4	5
Suzuki reaction Conversion (%)	100	96	89	72	48
Time (hrs)	2.5	2.5	2.5	2.5	2.5
Heck reaction Conversion (%)	100	88	74	55	31
Time (hrs)	18	18	18	18	18

5. Conclusions

In summary, we have successfully synthesized a novel PCA-GNS-Pd catalyst. The catalytic activity of this heterogeneous catalyst was investigated towards Suzuki-Miyaura and Heck-Mizoroki cross-coupling reactions in pure water. The catalyst exhibited high stability and reusability up to five cycles. The easy preparation of the catalyst, its excellent catalytic performance in an aqueous medium and easy recovery of the catalyst makes PCA-GNS-Pd a promising heterogeneous catalyst system for cross coupling reactions. The coupling of aryl chlorides and bromides under moderate reaction conditions can be achieved in water with or without the aid of PTC. Due to the amphiphilic nature of PCA-GNS-Pd material, it can be easily dispersible in water and therefore exhibits remarkably high, stable catalytic activity in water. Further, due to the presence of the carboxylic groups in this catalyst, intercalation and sorption of the Pd^{+2} ions on the PCA-GNS support is possible during the synthesis of this catalyst. This also allows the association of organic substrates to the catalyst during the catalytic reaction due to non covalent interaction of PCA. These nanocomposite materials can also be used for various industrial applications such as environmental protection, biomedical applications, electrocatalysis and sensors.

Supporting information: ^{1}H NMR and ^{13}C NMR spectra of products.

Acknowledgements
V.S. thanks CSIR and Acsir New Delhi for providing research fellowship. This work was supported by funding from DBT, Government of India. The authors thank Dr.M.Lakshmi Kantam, Director, IICT for the kind support and encouragement.

Notes
RMIT Centre, CSIR - Indian Institute of Chemical Technology, Hyderabad-500607, A.P. India.
*e-mail: sghosh@iict.res.in, fax: 9127160921, Phone: +91-40-27191385 (O), Fax: +91-40-27160921

References:

[1] X. Huang, X. Qi, F. Boeyab and H. Zhang, *Chem. Soc. Rev.,*2012, **41,** 666–686.

[2] V. Georgakilas, M. Otyepka, A. B. Bourlinos, V. Chandra, N. Kim, K. C. Kemp, P. Hobza, R. Zboril and K. S. Kim, *Chem. Rev.,* 2012, **112, 6156**−6214.

[3] A. K. Geim, *Science,* 2009, **324,** 1530−1534.

[4] A.K. Geim, *Nat. Mater.,* 2007, **6,** 183.

[5] J. Liu, J. Tanga and J. J. Gooding, *J. Mater. Chem.,* 2012, **22**, 12435–12452.

[6] K. S. Novoselov, A. K. Geim, S. V. Morozov, D. Jiang, M. L. Katsnelson, I. V. Grigorieva, S. V. Dubonos and A. A. Firsov, *Nature ,* 2005, **438,** 197−200.

[7] K.H. Lee, S.W. Han, K.Y. Kwon and J.B. Park, *J. Colloid Interface Sci*., 2013, **403,** 127- 33.

[8] O Metin, S. F. Ho, C. Alp, H. Can, M. N. Mankin, M. S. Gültekin, M. Chi and S. Sun, *Nano Res.,* 2013, **6(1)**, 10–18.

[9] C. Huang, C. Li and G. Shi, *Energy Environ. Sci.,* 2012, **5**, 8848–8868.

[10] G. Wu, X. Wang, N. Guan and L. Li, *Applied Cat. B: Environmental,* 2013, **136–137**, 177–185.

[11] S. Moussa, A. R. Siamaki, B. F. Gupton and M. S. El-Shall, *ACS Catal.,* 2012, **2**, 145−154.

[12] N. Zhang, Y. Zhang and Y. Xu, *Nanoscale*., 2012, **4**, 5792–5813.

[13] M. Yangab and Y. Xu, *Phys. Chem. Chem. Phys.,* 2013, 15, 19102—19118.

[14] M.Q. Yang, N. Zhang, M. Pagliaro, and Y.J. Xu, *Chem.Soc.Rev.,* 2014, DOI. 10.1039/c4cs00213j.

[15] M. Lamblin, L. Nassar-Hardy, J. C. Hierso, E. Fouquet, and F. X. Felpin, *Adv. Synth.Catal.,* 2010, **352**, 33–79.

[16] P. Veerakumara, M. Velayudham, K. L. Lub and S. Rajagopal, *Applied Catalysis A: General,* 2013, **455,** 247– 260.

[17] V. Polshettiwar and R. S. Varma, *Green Chem.,* 2010, **12,** 743−754.

[18] C. Putta and S. Ghosh, *Adv. Synth. Catal.,* 2011, **353**, 1889-1896.

[19] K. Qu, L. Wu, J. Ren and X. Qu, *ACS Appl. Mater. Interfaces,* 2012, 4**,** 5001−5009.

[20] B. F. Machado and P. Serp, *Catal. Sci. Technol.,* 2012, **2**, 54–75.

[21] S. Park, J. An, I. Jung, R.D. Piner, S.J. An, X. Li, A. Velamakanni and R.S. Ruoff, *Nano Lett.,* 2009, **9,** 1593.

[22] A. R. Siamaki, A. El Rahman, S. Khder, V Abdelsayed, M. S El-Shall and B. F Gupton, *J. Catal.,* 2011, 279**,** 1–11.

[23] S. L. Buchwald, *Acc. Chem. Res.,* 2008, **41,** 1439.

[24] L. Yin and J. Liebscher, *Chem. Rev.,* 2007, **107,** 133.

[25] X. An, T. Simmons, R. Shah, C. Wolfe, K. M. Lewis, M. Washington, S. K. Nayak,S. Talapatra and S. Kar**,** *Nano Lett.,* 2010, **10,** 4295–4301.

[26] N. Shang, C. Feng, H. Zhang, S. Gao, R. Tang, C. Wang and Z. Wang, *Catalysis Communications,* 2013, **40,** 111–115.

[27] S. S. Shendage, A. S. Singh and J. M. Nagarkar, *Tetrahedron Lett.,* 2014, **55,** 857–860.

[28] H. H. Zhang, B. Liu, J. Wang, K. Feng, B. Chen, C. H. Tung and L. Z. Wu, *Tetrahedron* 2014, 1-5

[29] S. S. Shendage, U. B. Patil and J. M. Nagarkar, *Tetrahedron Lett.,* 2013, **54,** 3457–3461

[30] N. Miyaura and A. Suzuki, *J. Chem. Soc., Chem. Commun*., 1979, 866–867.

[31] A. Suzuki, *Pure Appl. Chem.,* 1994, 66, 213–222.

[32] N. Miyaura, K. Yamada and A. Suzuki, *Tetrahedron Lett.,* 1979, 3437–3440.

[33] A. Suzuki, *Angew. Chem. Int. Ed.,* 2011, 50, 6722–6737.

[34] A. Suzuki and Y. Yamamoto, *Chem. Lett.,* 2011, **40**, 894–901.

[35] A. Fihri, M. Bouhrara, B. Nekoueishahraki, J. M. Basset and V. Polshettiwar, *Chem. Soc.Rev.,* 2011, **40**, 5181-5203.

[36] A. de Meijere and F. Meier, *Angew. Chem. Int. Ed. Engl.,*1994, **33**, 2379.

[37] I. P. Beletskaya and A. V. Cheprakov, *Chem. Rev.,* 2000, **100**, 3009-3066;

[38] V. Farina, *Adv. Synth. Catal.,* 2004, **346**, 1553-1582.

[39] N.Miyaura and A. Suzuki, *Chem. Rev.,*1995**, 95**, 2457–2483.

[40] Ö. Metin, E. Kayhan, S. Özkar and J.J. Schneider, *International Journal of Hydrogen Energy,* 2012, **37,** 8161–8169.

[41] Y. Li, Y. Yu, J. Wang, J. Song, Q. Li, M. Dong and C. Liu, *Applied Cat. B: Environmental.,* 2012, **125,** 189–196.

[42] R. Wang, Z. Wu, C. Chen, Z. Qin, H. Zhu, G. Wang, H. Wang, C. Wu, W. Dong, W. Fan and J. Wang, *Chem. Commun.,* 2013, **49,** 8250-8252.

[43] T. Maiyalagan, X Wanga and Manthiram, *RSC Adv.,* 2014, **4**, 4028–4033.

[44] Q. Wang, X. Cui, J. Chen, X. Zheng, C. Liu, T. Xue, H. Wang, Z. Jin, L. Qiao and W Zheng, *RSC Adv.,* 2012, **2,** 6245–6249.

[45] J.Yang, Y. Xie, R. Wang, B. Jiang, C.Tian, G. Mu, J. Yin, B. Wang and H. Fu, *ACS Appl. Mater.Interfaces.,* 2013 **5(14),** 6571–6579.

[46] N Morimoto,S Yamamoto, Y Takeuchia and Yuta Nishina, *RSC Adv.,* 2013, **3**, 15608– 15612.

[47] Z Wang, C Xu, G Gao and X Li, *RSC Adv.,* 2014, **4**, 13644–13651.

[48] M. Yang, X Pan, N Zhang and Y. Xu, *CrystEngComm.,* 2013, **15**, 6819– 6828.

[49] C. A. Fleckenstein and H. Plenio, *Chem. Eur. J.,* 2007, **13,** 2701–2716.

[50] A. Scarso and G. Strukul, *Adv. Synth. Catal.,* 2005, **347,** 1227-1234.

[51] R. Selke, J. Holz, A. Riepe and A. Bömer, *Chem. Eur. J.,* 1998, **4,** 769;

[52] A. Scarso, *Chem. Ind.,* 2009, **91**, 142**.**

[53] V. B. Parambhath, R. Nagar, K. Sethupathi and S. Ramaprabhu. *J. Phys. Chem. C.,*2011, **115,** 15679–15685.

[54].Y. Xu, H. Bai, G. Lu, C. Li and G. Shi, *J. Am. Chem. Soc.,* 2008, **130,** 5856-5857.

[55] B. Hu, T. Wu, K. Ding, X. Zhou, T. Jiang and B. Han, *J. Phys. Chem.C.,* 2010, **114,** 3396–3400.

[56] K. R. Priolkar, P. Bera, P. R. Sarode, M. S. Hegde, S. Emura, R. Kumashiro and N. P. Lalla, *Chem. Mater.,* 2002, **14,** 2120–2128.

[57] Y. Li, X. Fan, J. Qi, J. Ji, S. Wang, G. Zhang and F. Zhang, *Nano Res.,* 2010, **3,** 429–437.

[58] D. R. Dreyer, S. Park, C. W. Bielawski and R. S. Ruoff, *Chem.Soc. Rev.,* 2010, 39, 228.

[59] H. Huang and X. Wang, *J. Mater. Chem.,* 2012, **22**, 22533–22541.

[60] M. Zhang, Z. Yan, Q. Sun, J. Xie and J. Jing, *NewJ. Chem.,* 2012, **36**, 2533–2540.

[61] Y. Jiang, Y. Lu, F. Li, T. Wu, L. Niu and W. Chen, *Electrochemistry Communications.* 2012, **19**, 21–24.

[62] J. Amali and R. K. Rana, *Green Chem.,* 2009, **11,** 1781–1786;

[63] G. M. Scheuermann, L. Rumi, P. Steurer, W. Bannwarth and R. Muelhaupt, *J. Am.Chem. Soc.,* 2009, **131,** 8262–8270.